Paper

Int'l J. of Aeronautical & Space Sci. 15(1), 63–73 (2014)
DOI:10.5139/IJASS.2014.15.1.63

IJASS
International Journal of Aeronautical and Space Sciences

Research on Robust Stability Analysis and Worst Case Identification Methods for Parameters Uncertain Missiles

Zhenqian Hou* and Xiaogeng Liang**

Automation College, Northwestern Polytechnic University, Xi'an, China

Wenzheng Wang***

China Aerodynamics Research & Development Center, Mianyang, China

Abstract

For robust stability analysis of parameters uncertainty missiles, the traditional frequency domain method can only analyze each respective channel at several interval points within uncertain parameter space. Discontinuous calculation and couplings between channels will lead to inaccurate analysis results. A method based on the ν-gap metric is proposed, which is able to comprehensively evaluate the robust stability of missiles with uncertain parameters; and then a genetic-simulated annealing hybrid optimization algorithm, which has global and local searching ability, is used to search for a parameters combination that leads to the worst stability within the space of uncertain parameters. Finally, the proposed method is used to analyze the robust stability of a re-entry missile with uncertain parameters; the results verify the feasibility and accuracy of the method.

Key words: parameter uncertainty, robust stability, ν-gap metric, hybrid optimization

1. Introduction

As technology advances, missiles in modern warfare must have longer range, and higher maneuverability. These kinds of missiles will face severe changes of external environment, and perturbations of internal parameters in their flight envelope; meanwhile, complex aerodynamic layout will lead to serious couplings between the missiles' channels. Control system design for modern missiles therefore presents a challenge for control engineers. Control system stability and performance evaluation for missiles with uncertain parameters is an important part of control system design. Traditional frequency domain evaluation methods are carried out for the missiles' pitch, yaw, and roll channels, respectively, at discrete points, in uncertain parameters space. So the evaluation results have two problems: 1) due to discontinuous calculation in uncertain parameters space, the evaluation is not comprehensive, which may lead to inaccurate results; and 2) in the process of evaluation, along with the increased number of uncertain parameters, the time for calculation will increase exponentially, and the evaluation process will cost considerable time and manpower. Control system designers need to find out methods for evaluation that offer higher efficiency and accuracy.

"Gap" computes the gap metrics between two LTI objects. It gives a numerical value $\delta(P_0, P_1)$ between 0 and 1, for the distance between a nominal system P_0 and a perturbed system P_1. The gap metric was introduced into the control literature by Zames and El-Sakkary [1], and exploited by Georgiou and Smith [2, 3]. G. Vinnicombe puts forward the concept of the ν-gap metric because the gap metric is conservative[4]. Qui and Davidson proved that the generalized stability margins of a nominal system P_0, perturbation system P_1, and the gap metric (ν-gap metric) between two systems satisfy the triangle inequality relations [5]; while Keith Glover et al. gave the relationship between the generalized stability margin, and the traditional amplitude/phase stability margin [6].

* Ph. D Student
** Professor, Corresponding author: lxg@sina.com
*** Dr.

Received: December 11, 2013 Revised: February 22, 2014 Accepted: February 23, 2014

http://ijass.org pISSN: 2093-274x eISSN: 2093-2480

The genetic algorithm (GA) is a kind of stochastic global searching method, imitating the evolutionary process of selection, crossover and mutation in nature [7, 8]. The GA can search with extensive scope but is not easy to converge to the exact values of optimal solutions. The simulated annealing algorithm is a simulation of the annealing process in thermodynamics [9, 10]. At high temperature, the optimization process is carried out at the global level, while at low temperature, it tends to find more exact local solutions.

Based on the above theories, this paper puts forward a stability evaluation method that is based on the ν-gap metric for missiles with uncertain parameters. Firstly, the method calculates the lower bound of the generalized stability margin of the perturbation system, and quickly determines whether a system satisfies the stability margin index. Then, if the results don't meet the stability requirements, a hybrid optimization algorithm is used to search for the combination of uncertain parameters that leads to the worst case. Designers can improve control systems, according to the evaluation results.

2. The Stability of Feedback Systems

2.1 The Internal Stability

A closed-loop system [*P*, *C*] is shown in Figure 1. In the figure, *u* and *y* denote the inputs and outputs of the closed-loop system, *d* and *n* are the output noise of controller and measurements noise, respectively. From *d* and *n* to *y* and *u*, the closed-loop transfer function matrix can be expressed as:

$$G_{P,C}=\begin{bmatrix}P\\ I\end{bmatrix}(I+CP)^{-1}\begin{bmatrix}I & C\end{bmatrix} \tag{1}$$

If the four transfer functions in equation (1) are stable, it is said that closed-loop system [*P*, *C*] is internally stable, which means the closed-loop system is stable.

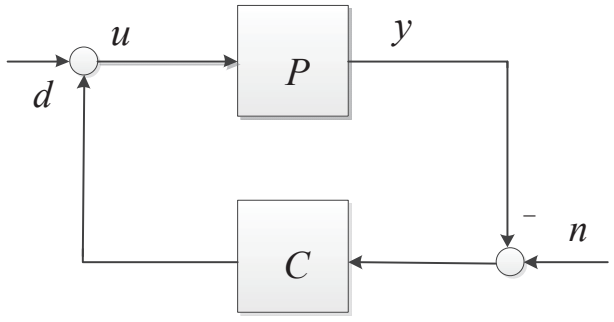

Fig. 1. Feedback Control System Structure

2.2 Generalized Stability Margin

If the closed-loop system [*P*, *C*] is stable, the frequency domain generalized stability margin of the closed-loop system is defined as:

$$\rho\left(P(j\omega),C(j\omega)\right)=1/\bar{\sigma}\left(G_{P,C}(j\omega)\right) \tag{2}$$

The generalized stability margin of the closed-loop system is then defined as:

$$b_{P,C}:=\begin{cases}\inf\limits_{\omega}\rho\left(P(j\omega),C(j\omega)\right) & [P,C]\text{ is stable}\\ 0 & \text{else}\end{cases} \tag{3}$$

$b_{P,C}$ is a value between 0 and 1. When the norm of the closed-loop system transfer function matrix is small, $b_{P,C}$ is large, else $b_{P,C}$ is small.

It is possible to relate $b_{P,C}$ to the classical gain and phase margins. For a stable SISO system [*P*, *C*], define the gain and phase margins as follows:

If $pc(j\omega)\in R^{+}$ for some ω, then

$$GM(p,c):=\min_{k\in R,k\geq 1}\{k:kpc(j\omega)=-1 \text{ or } pc(j\omega)/k=-1,$$

otherwise, $GM(p,c):=\infty$.

If $|pc(j\omega)|=1$ for some ω, then

$$PM(p,c):=\min_{\varphi\in R,\varphi\geq 0}\{\varphi:e^{j\varphi}pc(j\omega)=-1 \text{ or } e^{-j\varphi}pc(j\omega)=-1 \text{ for some } \omega\},$$

otherwise, $PM(p,c):=\infty$.

Theorem 1: If [*P*, *C*] is stable, then $GM(p,c)\geq(1+b_{p,c})/(1-b_{p,c})$, and $PM(p,c)\geq 2\arcsin(b_{p,c})$.

PROOF: According to equation (3), we have

$$|1+pc|/\sqrt{1+|p|^2}\sqrt{1+|c|^2}\geq b_{p,c},\forall\omega \tag{4}$$

So, at frequencies where the gain margin is *k*, $pc(j\omega)=-1/k\in R^{+}$, then

$$(1-1/k)^2\geq b_{p,c}^2\left(1+|p|^2\right)\left(1+1/k^2|p|^2\right)\geq b_{p,c}^2\left(1+1/k\right)^2 \tag{5}$$

The gain margin result is obtained from equation (5).

Similarly, at frequencies where the phase margin is φ, $pc(j\omega)=-e^{-j\varphi}$, and

$$\left|1-1/e^{j\varphi}\right|^2=4\sin^2(\varphi/2)\geq b_{p,c}^2\left(1+|p|^2\right)\left(1+1/|c|^2\right)\geq 4b_{p,c}^2 \tag{6}$$

The phase margin result is then obtained from equation (6).

END.

The generalized stability margin of multivariable systems also makes sense. First, we introduce the following Proposition [11]:

Proposition: Let $\triangle_1$ and $\triangle_2$ be complex diagonal matrices, which perturb a nominal plant P to $P_\triangle=(I+\triangle_1)P(I+\triangle_2)^{-1}$. If $\rho_{W_o P W_i, W_i^{-1} C W_o^{-1}} \geq \beta$ for any diagonal input and output analysis weights, W_i and W_o, then $[P_\triangle, C]$ is stable for any perturbations satisfying $\|\Delta_1\|_\infty < \beta$ and $\|\Delta_2\|_\infty < \beta$.

For a given $\beta \in [0,1)$, the perturbation plant $P_\triangle=(I+\triangle_1)P(I+\triangle_2)^{-1}$ (see Figure 2) can be written as:

$$P_\Delta = \frac{1}{\sqrt{1-\beta^2}}(I+\Delta_1)P(I-\Delta_2)^{-1}\sqrt{1-\beta^2} \tag{7}$$

Note that the sets $\left\{\frac{1+\delta_1}{\sqrt{1-\beta^2}} : |\delta_1| < \beta\right\}$ and $\left\{\frac{\sqrt{1-\beta^2}}{1-\delta_2} : |\delta_2| < \beta\right\}$ are identical; therefore, the result in Proposition is equivalent to saying that each input and output can be independently and simultaneously perturbed by a term $\delta_{io} \in \left\{\frac{1+\delta}{\sqrt{1-\beta^2}} : |\delta| < \beta\right\}$. This set of complex gain/phase offsets describes a region of allowable input/output multiplicative perturbations δ_{io}, which satisfy:

$$\left(\mathrm{Re}(\delta_{io}) - \frac{1}{\sqrt{1-\beta^2}}\right)^2 + (\mathrm{Im}(\delta_{io}))^2 < \frac{\beta^2}{(1-\beta^2)} \tag{8}$$

Equation (8) describes a permissible input/output disturbance area. For example, when β=0.2, each input and output gain changes less than $\sqrt{\frac{1+\beta}{1-\beta}} \approx 1.22(1.73dB)$, respectively; or the phase change is less than $\left(\beta/\sqrt{1+\beta^2}\right) \approx 11.3°$, respectively, and the perturbation system remains stable.

2.3 The Weighted Generalized Stability Margin

The proposition shows that we need to apply weights, in order to assess the generalized stability margin $b_{P,C}$ of a specified closed-loop system. Since the plant and controller are fixed, the loop shape must not be altered by the weights. So we apply input and output weights, in the way shown in Figure 3.

The frequency domain weighted generalized stability margin of the system can be obtained as:

$$\rho_{weight}\left(P(j\omega), C(j\omega)\right) = 1/\bar{\sigma}\left(\begin{bmatrix} W_o & \\ & W_i^{-1} \end{bmatrix} G_{P,C}(j\omega) \begin{bmatrix} W_o^{-1} & \\ & W_i \end{bmatrix}\right) \tag{9}$$

The frequency domain optimal weighted generalized stability margin is:

$$\rho_{bw}\left(P(j\omega), C(j\omega)\right) = \max_{W_i, W_o} \rho\left(W_o P(j\omega) W_i, W_i^{-1} C(j\omega) W_o^{-1}\right) \tag{10}$$

The optimal weighted generalized stability margin of the closed-loop system is then:

$$b_{bw(P,C)} := \begin{cases} \min_\omega \rho_{bw}\left(P(j\omega), C(j\omega)\right) & [P, C] \text{ is stable} \\ 0 & \text{else} \end{cases} \tag{11}$$

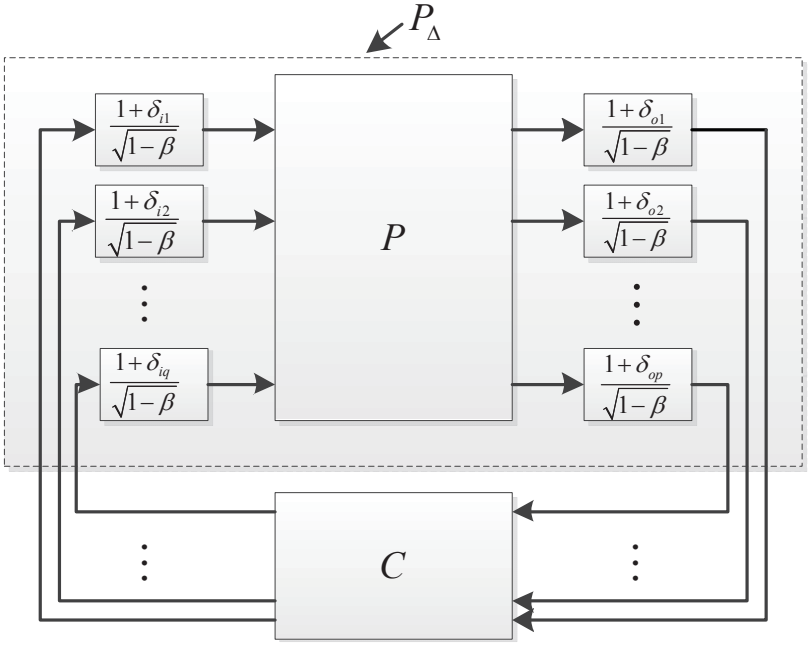

Fig. 2. Input/Output Perturbations for Multi-Loop Systems

The problem of finding the optimal weights is a convex optimization problem, which can be solved by an optimization algorithm. So the optimal generalized stability margin of the closed-loop system can be calculated at frequency points, and minimum value can be seen as a measurement of the closed-loop system robustness to input/output perturbations.

3. The ν-gap Metric

Define the ν-gap metric $\delta_\nu(P_1, P_2)$ between systems P_1 and P_2 [11], as follows:

$$\delta_\nu(P_1,P_2)=\begin{cases}\left\|\left(I+P_2P_2^*\right)^{-1/2}\left(P_2-P_1\right)\left(I+P_1^*P_1\right)^{-1/2}\right\|_\infty & \text{if } p[P_2,P_1^*]=p[P_1,P_1^*]\\ 1 & \text{else}\end{cases} \quad (12)$$

where, $p[P_2, P_1^*]$ denotes the number of open RHP poles of the fictitious feedback system, comprising the plants P_2 and P_1^*. P_1^* is the conjugate transpose of P_1. The ν-gap metric quantifies the difference between the two systems, and its scope is within [0, 1].

The frequency domain ν-gap metric can be expressed as:

$$\kappa\left(P_1(j\omega),P_1(j\omega)\right)=\bar{\sigma}\left(\left(I+P_2P_2^*\right)^{-1/2}\left(P_2-P_1\right)\left(I+P_1^*P_1\right)^{-1/2}\right)(j\omega) \quad (13)$$

So that:

$$\delta_\nu(P_1,P_2)=\max_\omega \kappa\left(P_1(j\omega),P_2(j\omega)\right) \quad (14)$$

Reference [12] proves that the ν-gap metric between systems P_1 and P_2 satisfies the mathematical definition of distance. Importantly, it satisfies the triangle inequality; so if P_2 is the result of perturbing P_0 to P_1, and then P_1 to P_2, then:

$$\delta_\nu(P_0,P_2)\le\delta_\nu(P_0,P_1)+\delta_\nu(P_1,P_2) \quad (15)$$

That is to say, the ν-gap metric between P_0 and P_2 is equal to, or less than the sum of the effects of the individual perturbations.

4. The Robust Stability of the Feedback System

4.1 Relationships between the Generalized Stability Margin and the ν-gap Metric

Before introducing the relationship between the generalized stability margin and the ν-gap metric, we first introduce the following theorem(theorem 2) [12].

For any plants P_1 and P_2 within a set and controller C, the following relationship exists:

$$\arcsin b_{P_2,C}\ge\arcsin b_{P_1,C}-\arcsin\delta_\nu\left(P_1,P_2\right) \quad (16)$$

Equation (16) can be simplified as [12]:

$$b_{P_2,C}\ge b_{P_1,C}-\delta_\nu\left(P_1,P_2\right) \quad (17)$$

From equation (17), it can be seen that within a system set, if $b_{P_1, C}$ is large and $\delta_\nu(P_1,P_2)$ is small, then $b_{P_2, C}$ is also large. So we can say $b_{P, C}$ indicates the robust stability of the feedback system.

When using $b_{P, C}$ for system stability analysis, the input/output weights are introduced; so later in this article, the ν-gap metric between plants P_1 and P_2 refers to the distance between the weighted plants.

4.2 Robust Stability Analysis Method

We can use the ν-gap metric to calculate the influence of each parameter on the stability of feedback systems, and the lower bound of the frequency domain generalized stability margin of parameter uncertain systems can also be calculated, using the relationship between the generalized stability margin, and the ν-gap metric.

According to equation (15) and equation (17), the lower bound of the frequency domain optimal generalized stability margin of the uncertain parameters system $P_\Delta, \Delta=\{\delta_1,\delta_2,\cdots,\delta_n\}$ is:

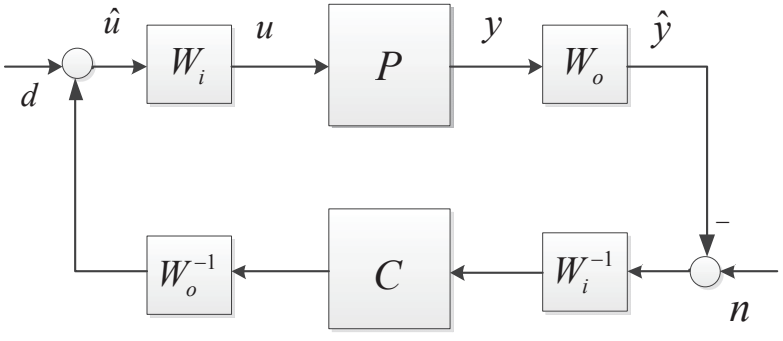

Fig. 3. Feedback System with Weighting Matrices

$$\rho_{bw}\left(P_{\Delta}(j\omega),C(j\omega)\right)\geq\rho_{bw}\left(P_0(j\omega),C(j\omega)\right)-\sum_{i=1}^{n}\kappa\left(P_{i-1}(j\omega),P_i(j\omega)\right) \quad (18)$$

The lower bound of the optimal generalized stability margin is:

$$b_{bw(P,C)}=\min_{\omega}\rho_{bw}\left(P_{\Delta}(j\omega),C(j\omega)\right) \quad (19)$$

According to equation (18) and equation (19), the robust stability of parameters uncertain systems can be rapidly evaluated. When the robust stability does not meet the requirements, the optimization algorithm can be used to search for the uncertain parameters combination that leads to the worst case.

5. Genetic-Simulated Annealing Hybrid Optimization Algorithm

5.1 Genetic Algorithm

The genetic algorithm is a method for solving both constrained and unconstrained optimization problems, which is based on natural selection, the process that drives biological evolution. The genetic algorithm repeatedly modifies a population of individual solutions. At each step, the genetic algorithm selects individuals at random from the current population to be parents, and uses them to produce the children for the next generation. Over successive generations, the population "evolves" toward an optimal solution. The genetic algorithm can be applied to solve a variety of optimization problems that are not well suited to standard optimization algorithms, including problems in which the objective function is discontinuous, non-differentiable, stochastic, or highly nonlinear.

The genetic algorithm uses three main types of rules at each step, to create the next generation from the current population:

1) Selection rules select the individuals(called parents). They contribute to the population at the next generation.

2) Crossover rules combine two parents, to form children for the next generation.

3) Mutation rules apply random changes to individual parents, to form children.

5.2 Simulated Annealing Algorithm

Simulated annealing is a method for solving unconstrained and bound-constrained optimization problems. The method models the physical process of heating a material, and then slowly lowering the temperature to decrease defects, thus minimizing the system energy.

At each iteration of the simulated annealing algorithm, a new point is randomly generated. The distance of the new point from the current point, or the extent of the search, is based on a probability distribution with a scale proportional to the temperature. The algorithm accepts all new points that lower the objective; but also, with a certain probability, points that raise the objective. By accepting points that raise the objective, the algorithm avoids being trapped in local minima, and is able to explore globally for more possible solutions. An annealing schedule is selected to systematically decrease the temperature, as the algorithm proceeds. As the temperature decreases, the algorithm reduces the extent of its search, to converge to a minimum.

Consider the following optimization problem:

$$f: x\rightarrow R^{+} \quad (20)$$

where, $x\in S$ is a feasible solution to the optimization problem, and S is the definition domain, $R^{+}=\{y\,|\,y\in R, y>0\}$. $N(x)\subseteq S$ is a neighborhood of x.

First, give an initial temperature T_0, and an initial feasible solution $x(0)$ of the optimization problem, and use $x(0)$ to generate $x'\in N(x(0))$. Whether or not x' is accepted as a new solution, depends on the probability, as follows:

$$P(x(0)\rightarrow x')=\begin{cases}1, & if \quad f(x')<f(x(0))\\ e^{-\frac{f(x')-f(x(0))}{T_0}}, & others\end{cases} \quad (21)$$

After some iterations at the current temperature, decrease the temperature to T_i, and repeat the above process, until reaching the minimum temperature.

At high temperature, the simulated annealing algorithm carries out the optimization at global scope; at low temperature, it tends to find local optimal solutions. The calculation is not parallel, so the optimization process is slow.

5.3 The Genetic-Simulated Annealing Hybrid Optimization Algorithm

The genetic algorithm searches at global scope by parallel calculating; but is not easy for it to converge to the exact optimal solution. The simulated annealing algorithm is able to find a more accurate solution, but the optimization process is slow. According to the characteristics of these two algorithms, we construct the hybrid genetic-simulated annealing algorithm (GA-SA), by combining these two algorithms. First, given the initial population, the genetic algorithm is used to find out the approximated optimal solutions at global scope; then the simulated annealing algorithm searches in the neighborhood of approximate

solutions, to find a more accurate optimal solution. The algorithm process is shown in Figure 4.

5.4 Optimization Algorithm Verification

In this section, four test functions are presented, to compare the computing performance of the hybrid algorithm (GA-SA), and the genetic algorithm (GA). The conditions of the two algorithms are the same, such as the populations, and length of an individual. The results are shown in Table 1. As we can see, under the same parameter settings, the genetic-simulated annealing hybrid algorithm

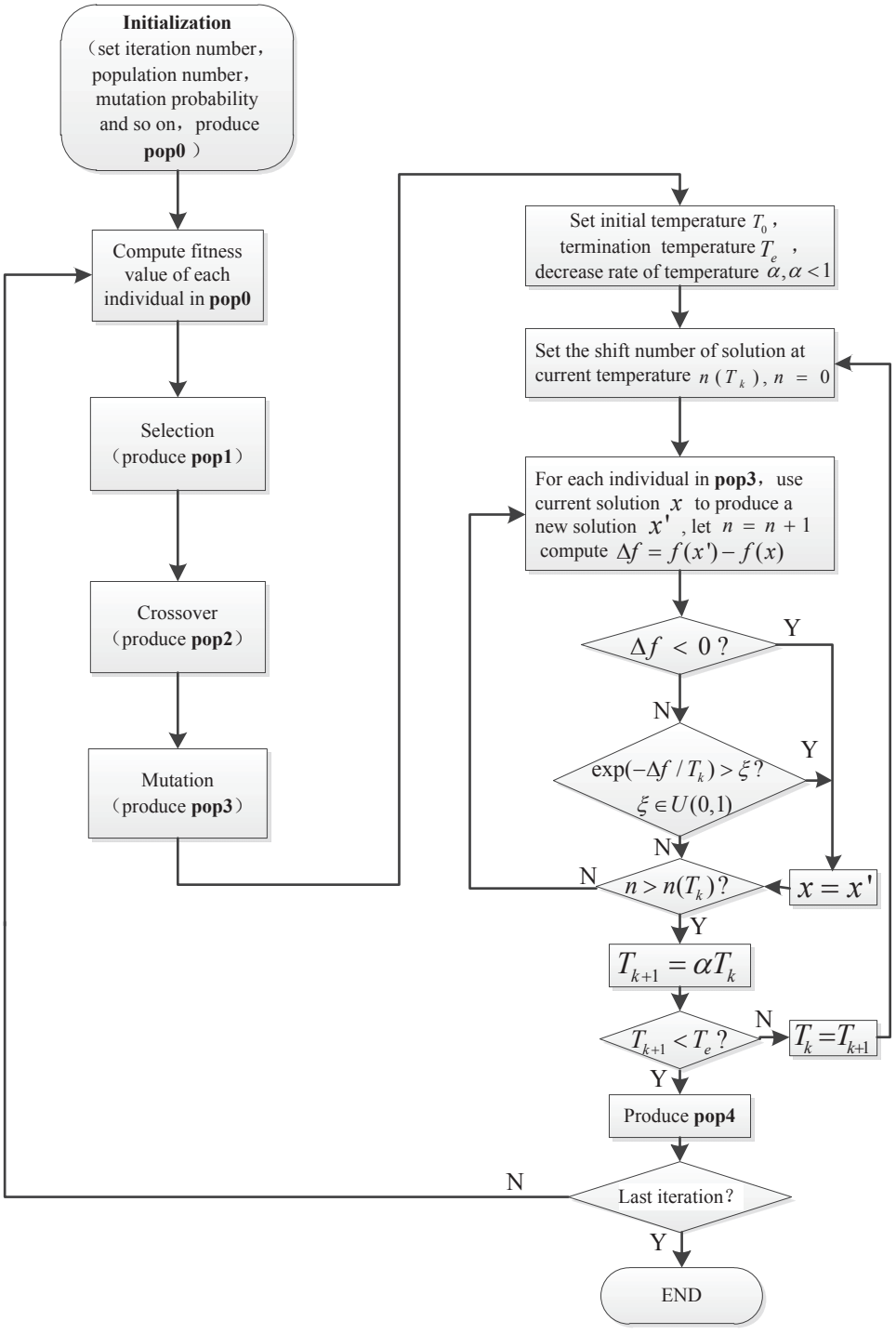

Fig. 4. Hybrid Optimization Algorithm Flow Diagram

is able to obtain more accurate results. The hybrid algorithm has faster convergence speed, and can always converge to more accurate optimal solutions. Compared with the genetic algorithm, the results show that the hybrid algorithm has more advantages, in terms of computational efficiency, and computational accuracy.

Test function (1):

$$f_1(x_1,x_2)=[1+(x_1+x_2+1)^2(19-14x_1+3x_1^2-14x_2+6x_1x_2+3x_2^2)]\times [30+(2x_1-3x_2)^2\times(18-32x_1+12x_1^2+48x_2-36x_1x_2+27x_2^2)]$$

Definition domain: $S=\{x\in R^2\,|-2\le x_i\le 2, i=1,2\}$

Test function (2):

$$f_2(x_1,x_2)=(x_2-5.1/(4\pi^2)x_1^2+5/\pi x_1-6)^2+10(1-1/(8\pi))\cos(x_1)+10$$

Definition domain: $S=\{x\in R^2\,|-5\le x_1\le 10, 0\le x_2\le 15\}$

Test function (3):

$$f_3(x)=10^5x_1^2+x_2^2-(x_1^2+x_2^2)^2+10^{-5}(x_1^2+x_2^2)^4$$

Definition domain: $S=\{x\in R^2\,|0\le x_i\le 20, i=1,2\}$

Test function (4):

$$f_4(x)=x_1^2+x_2^2$$

Definition domain: $S=\{x\in R^2\,|-1\le x_i\le 1, i=1,2\}$

6. Robust Stability Analysis of Missile with Uncertain Parameters

The linearized rigid-body model of a missile can be expressed by the state-space equations, as follows:

$$\begin{bmatrix}\dot\alpha\\ \dot\omega_z\\ \dot\beta\\ \dot\omega_y\\ \dot\omega_x\end{bmatrix}=\begin{bmatrix}Y^{\alpha} & Y^{\omega_z} & Y^{\beta} & Y^{\omega_y} & Y^{\omega_x}\\ M^{\alpha} & M^{\omega_z} & M^{\beta} & M^{\omega_y} & M^{\omega_x}\\ Z^{\alpha} & Z^{\omega_z} & Z^{\beta} & Z^{\omega_y} & Z^{\omega_x}\\ N^{\alpha} & N^{\omega_z} & N^{\beta} & N^{\omega_y} & N^{\omega_x}\\ L^{\alpha} & L^{\omega_z} & L^{\beta} & L^{\omega_y} & L^{\omega_x}\end{bmatrix}\begin{bmatrix}\alpha\\ \omega_z\\ \beta\\ \omega_y\\ \omega_x\end{bmatrix}+\begin{bmatrix}Y^{\delta_x} & Y^{\delta_y} & Y^{\delta_z}\\ M^{\delta_x} & M^{\delta_y} & M^{\delta_z}\\ Z^{\delta_x} & Z^{\delta_y} & Z^{\delta_z}\\ N^{\delta_x} & N^{\delta_y} & N^{\delta_z}\\ L^{\delta_x} & L^{\delta_y} & L^{\delta_z}\end{bmatrix}\begin{bmatrix}\delta_x\\ \delta_y\\ \delta_z\end{bmatrix}=Ax+Bu \quad (22)$$

$$\begin{bmatrix}\omega_x\\ \omega_y\\ \omega_z\end{bmatrix}=\begin{bmatrix}0 & 0 & 0 & 0 & 1\\ 0 & 0 & 0 & 1 & 0\\ 0 & 1 & 0 & 0 & 0\end{bmatrix}\begin{bmatrix}\alpha\\ \omega_z\\ \beta\\ \omega_y\\ \omega_x\end{bmatrix}=Cx$$

where, $x=[\alpha\ \omega_z\ \beta\ \omega_y\ \omega_x]^T$ is the state vector, α, ω_z, β, ω_y, ω_x are the angle of attack, pitch rate, angle of sideslip, yaw rate, and roll rate, respectively; $u=[\delta_x\ \delta_y\ \delta_z]^T$ is the input vector, δ_x, δ_y, δ_z are the elevator deflection, rudder deflection, and aileron deflection, respectively; and $y=[\omega_x\ \omega_y\ \omega_z]^T$ is the output vector.

The control system of the pitch channel is shown in Figure 5. n_z and n_{zc} are the normal overload and normal overload

Table 1. Comparison between the Two Algorithms

Test Function	Standard Solution	Algorithms	Mean Optimal Solution
f_1	(0 , -1)	GA	(-0.0001 , -1.0161)
		GA-SA	(0 ,-1)
f_2	$(\pi, 2.275)$	GA	(3.1537 , 2.2230)
		GA-SA	(3.1416 , 2.2750)
f_3	(0 , -15)	GA	(0.0019 , 14.8422)
		GA-SA	(0 , -14.9468)
f_4	(0 , 0)	GA	(-0.0009 , -0.0007)
		GA-SA	(0 , 0)

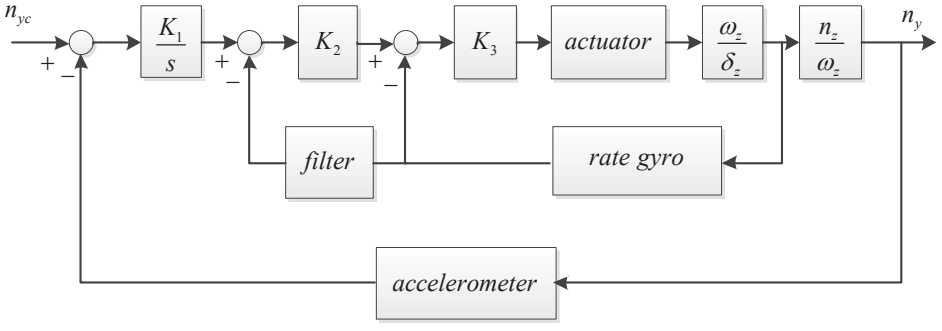

Fig. 5. The Control System of the Pitch Channel

command, respectively. K_1, K_2, K_3 are control variables.

The yaw channel is similar to the pitch channel.

The control system of the roll channel is shown in Figure 6. γ and γ_c are the roll angle and roll angle command, respectively. K_{r1}, K_{r2} are control variables.

The pitching moment derivative due to elevator deflection $C_m^{\delta_z}$, yawing moment derivative due to rudder deflection $C_n^{\delta_y}$, and rolling moment derivative due to aileron deflection $C_l^{\delta_x}$, are uncertain parameters, and their respective nominal values and variation ranges are shown in Table 2. The influence of each uncertain parameter on the stability of the closed-loop missile is calculated at a flight height of 4000 m, and speed of 2 Ma, using the ν-gap metric method. The state matrix A and control matrix B at a flight height of 4000 m, and speed of 2 Ma, are as follows:

$$A=\begin{bmatrix} -0.80 & 1 & -0.10 & 0 & 0 \\ -142 & 0.40 & 1.30 & -0.10 & -0.02 \\ 0.10 & 0 & -0.30 & 1 & 0 \\ 0 & 0.10 & -150 & -0.20 & 0 \\ 0 & 0.01 & -1200 & 0 & -2.56 \end{bmatrix}$$

$$B=\begin{bmatrix} -0.01 & 0.001 & -0.07 \\ -7.16 & 5.06 & 29730*C_m^{\delta_z} \\ -0.01 & -0.08 & 0 \\ -21.50 & 29290*C_n^{\delta_y} & 0 \\ 571420*C_l^{\delta_x} & -572 & 0 \end{bmatrix} \quad (23)$$

Case 1: only take $C_m^{\delta_z}$ as the uncertain parameter, and calculate the ν-gap metrics when the real values vary -10%, -5%, 5%, and 10% from the nominal value of $C_m^{\delta_z}$, respectively;

Case 2: only take $C_n^{\delta_y}$ as the uncertain parameter, and calculate the ν-gap metrics when the real values vary -10%, -5%, 5%, and 10% from the nominal value of $C_n^{\delta_y}$, respectively; and

Case 3: only take $C_l^{\delta_x}$ as the uncertain parameter, and calculate the ν-gap metrics when the real values vary -10%, -5%, 5%, and 10% from the nominal value of $C_l^{\delta_x}$, respectively.

Figures 7~9 show the ν-gap metrics between the nominal system and perturbed systems (perturbed as Case 1, Case 2 and Case 3). It can be seen that when the real value varies -10% from its nominal value, the uncertain parameter has the biggest influence on the stability of the closed-loop system. Let the real value vary -10% for each uncertain parameter; then from Figure 10, we can see that $C_n^{\delta_y}$ has bigger influence on the stability of the closed-loop system, than do $C_m^{\delta_z}$ and $C_l^{\delta_x}$.

All of the uncertain parameters are taken into consideration, to evaluate whether the missile's control system satisfies the stability requirements. The generalized stability margin index of the closed-loop system is defined as $b_{(P,\,C)}$=0.2. If the requirements are not satisfied, the generalized stability margin (as equation (11) shows) is taken as the objective function; then the GA-SA hybrid optimization algorithm is used to search for the uncertain parameters combination that leads to the worst performance. Figure 11 shows the generalized stability margin of the nominal system (solid line), and lower bound of the frequency domain generalized stability margin of the perturbed closed-loop system (dashed line), as well as the generalized stability margin of the worst case of the closed-loop system (dotted line).

Table 2 shows the uncertain parameters combination of worst case. It can be seen that when all the uncertain parameters vary 10% from the nominal values, their combination will lead to the worst performance. Comparing

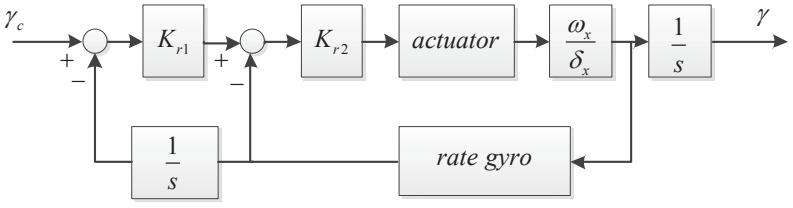

Fig. 6. The Control System of the Roll Channel

Table 2. Uncertain Parameters and the Worst Case Combination

Uncertain parameters	Nominal value (1/rad)	Variation range (%)	Worst case combination (1/rad)
$C_m^{\delta_z}$	-0.0064	[-10,10]	-0.00704
$C_n^{\delta_y}$	-0.0085	[-10,10]	-0.00935
$C_l^{\delta_x}$	-0.0027	[-10,10]	-0.00297

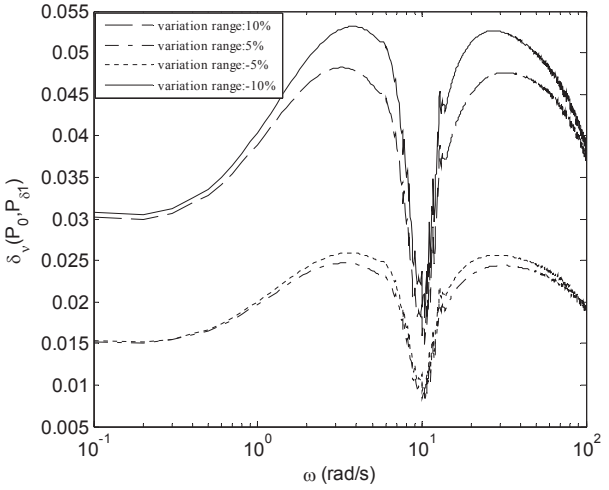

Fig. 7. *v*-Gap Metric between the Nominal and Perturbed Systems: Case 1

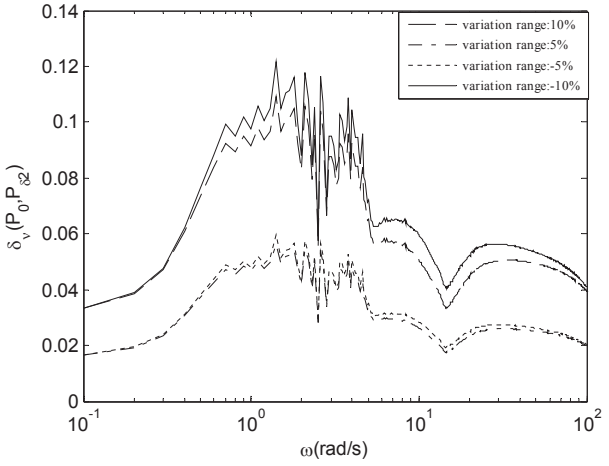

Fig. 8. *v*-Gap Metric between the Nominal and Perturbed Systems: Case 2

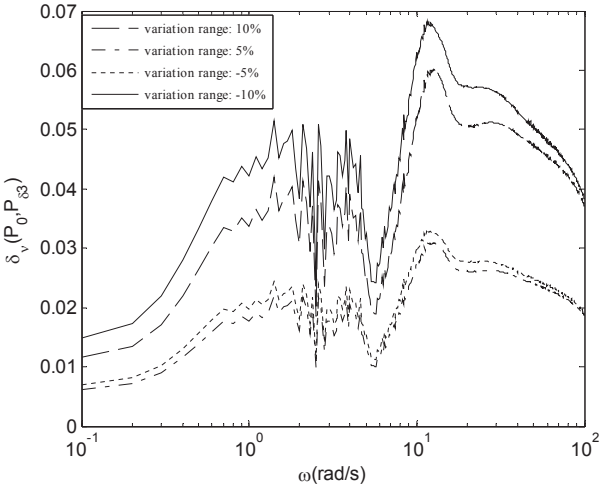

Fig. 9. *v*-Gap Metric between the Nominal and Perturbed Systems: Case 3

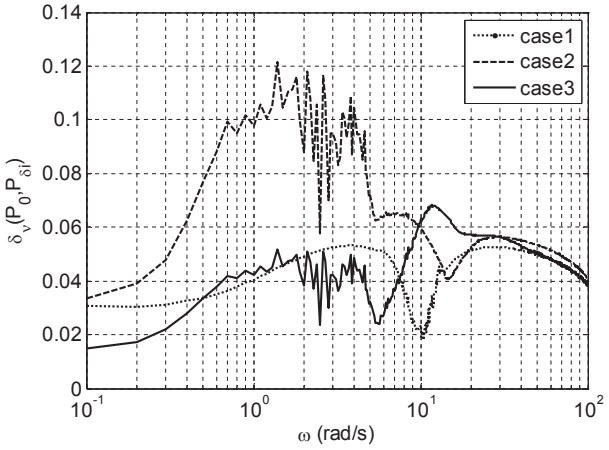

Fig. 10. *v*-Gap Metric between the Nominal and Perturbed Systems

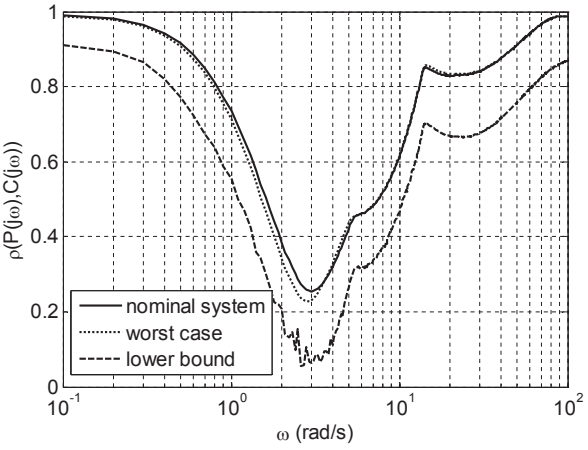

Fig. 11. Generalized Stability Margin and Lower Bound of the System

this with the results of Case 1, Case 2 and Case 3, it should be noted that while each uncertain parameter has the biggest influence on the stability of the closed system, their combination cannot be guaranteed to lead to the worst performance.

The traditional Nyquist stability criterion for the stability analysis of parameters uncertainty missiles is used to compare with the proposed method in this paper. The Nyquist stability criterion can only deal with the stability of an SISO system, so only one channel of the missile can be analyzed at a time. Many combinations of the uncertain parameters need to be tested, to get the worst performance; and the reliability of the results cannot be guaranteed, due to the limitation that is mentioned above. This especially applies for missiles with severe couplings between channels. Letting all uncertain parameters vary -10% / 10% from the nominal values at the same time, the stability analysis results of the pitch/yaw/roll channels are given in Figures 12~17, respectively. From Figures 12~17, we can see that the

combination in which all uncertain parameters vary 10%, has more influence on the stability of the missile, than the ones that vary -10%. Although each channel of the parameter-uncertain missile is stable, the stability of the whole missile cannot be guaranteed, due to the couplings between the channels.

6. Conclusions

In this paper, a method based on the *ν-gap* metric is proposed, to evaluate the robust stability of missiles with uncertain parameters. A genetic-simulated annealing hybrid optimization algorithm is proposed, to search for a parameters combination that leads to the worst performance, within the space of uncertain parameters. The results show that the importance of each uncertain parameter to the stability of the closed-loop system can be quantified through the ν-gap metric between the nominal system and the perturbed system; and the uncertain parameters combination leading to the worst performance is obtained, using the GA-SA hybrid optimization algorithm. Compared with the traditional method for robust stability analysis of parameters uncertainty missiles, the method proposed in this paper has higher calculation efficiency and accuracy.

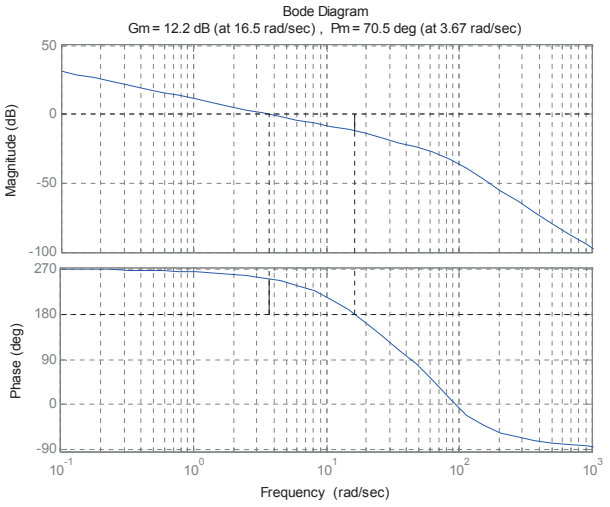

Fig. 12. The Stability of the Missile's Pitch Channel: Uncertain Parameters Vary 10%

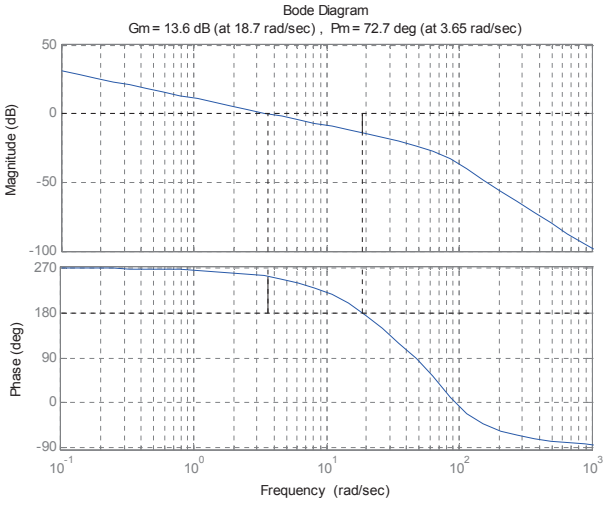

Fig. 13. The Stability of the Missile's Pitch Channel: Uncertain Parameters Vary -10%

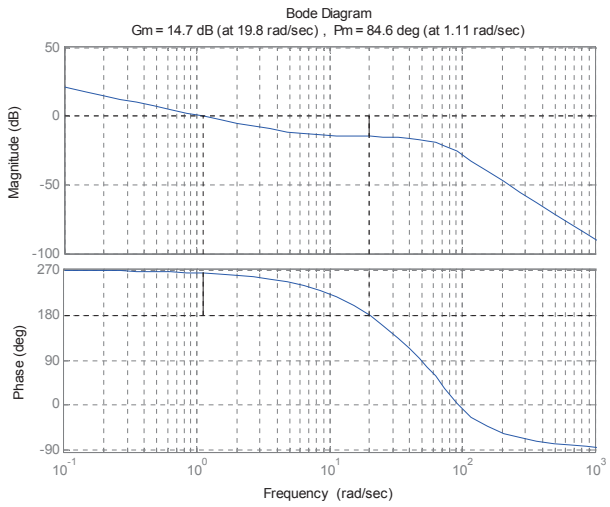

Fig. 14. The Stability of the Missile's Yaw Channel: Uncertain Parameters Vary 10%

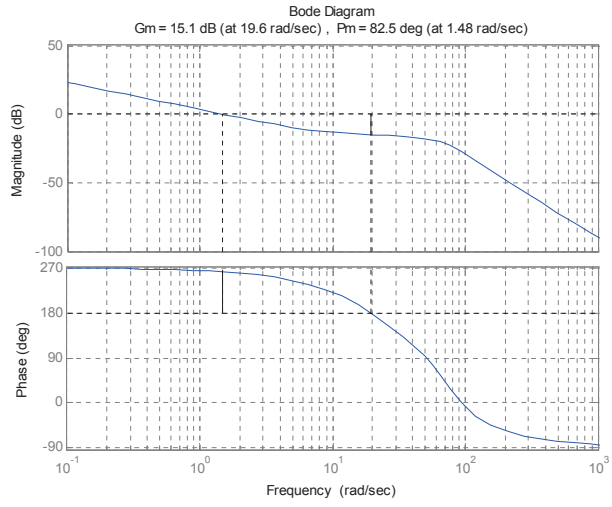

Fig. 15. The Stability of the Missile's Yaw Channel: Uncertain Parameters Vary -10%

DOI:10.5139/IJASS.2014.15.1.63

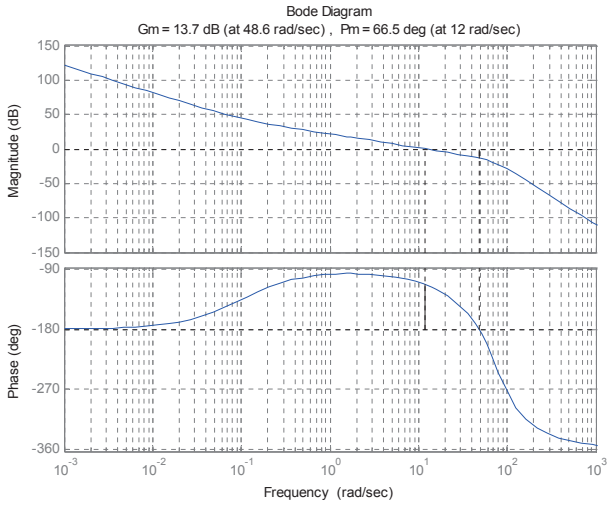

Fig. 16. The Stability of the Missile's Roll Channel: Uncertain Parameters Vary 10%

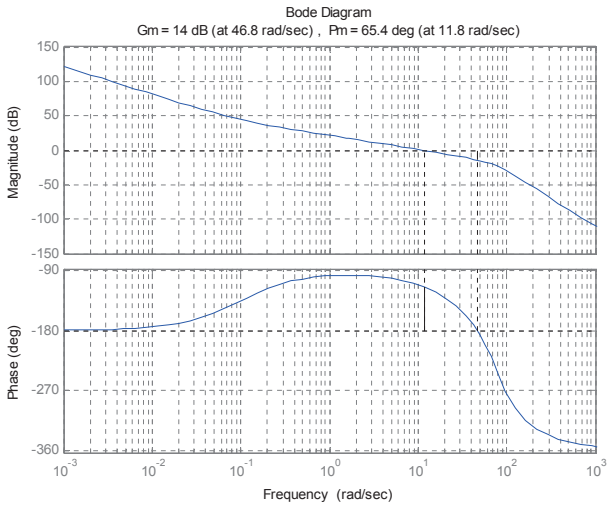

Fig. 17. The Stability of the Missile's Roll Channel: Uncertain Parameters Vary -10%

References

[1] El-Sakkary, "The gap metric: Robustness of stabilization of feedback systems", *IEEE Transactions on Automatic Control*, Vol.30, issue 3, 1985, pp. 240-247.

[2] Georgiou, T.T., A., "On the computation of the gap metric", *Systems Control Letters*, Vol. 11, issue 4, 1988, pp. 253-257.

[3] Georgiou, T.T. and M, smith, "Optimal robustness in the gap metric", *IEEE Transactions on Automatic Control*, Vol. 35, issue 6,1990, pp. 673-686.

[4] G. Vinnicombe, *Measuring Robustness of Feedback Systems*, PhD Dissertation, Department of Engineering, University of Cambridge, London, 1993.

[5] L. Qiu, and E.J. Davison, "Feedback stability under simultaneous gap metric uncertainties in plant and controller", *Systems Control Letters*, Vol. 18, issue 1, 1992, pp. 9-22.

[6] K. Glover, G. Vinnicombe, and G. Papageorgiou, "Guaranteed multi- loop stability margins and the gap metric", *Proceedings of 39th IEEE Conference on Decision and Control*, Sydney , Australia, 2000.

[7] Pengfei Guo, Xuezhi Wang, and Yingshi Han, "The Enhanced Genetic Algorithms for the Optimization Design", *2010 3rd International Conference on Biomedical Engineering and Informatics*, Yantai, China, 2010.

[8] Kyriaki Gkoutioudi, and Helen D. Karatza, A simulation study of multi-criteria scheduling in grid based on genetic algorithms. *2012 10th IEEE International Symposium on Parallel and Distributed Processing with Applications*, 2012.

DOI: 10.1109/ISPA.2012.48

[9] A. V. Kalashnikov, and V. A. Kostenko, "A Parallel Algorithm of Simulated Annealing for Multiprocessor Scheduling", *Journal of Computer and Systems Sciences International*, Vol. 47, No. 3, 2008, pp. 455–463.

[10] A. P. Cisilino, and B. Sensale, "Application of a simulated annealing algorithm in the optimal placement of the source points in the method of the fundamental solutions", *Computational Mechanics*, Vol. 28, issue 2, 2002, pp.129-136.

[11] Christopher Fielding, Andras Varga, Samir Bennani et al, *Advanced Techniques for Clearance of Flight Control Laws*, Springer, Berlin, 2002.

[12] G. Vinnicombe, *Uncertainty and Feedback: H-infinity loop-shaping and the nu-gap metric*, Imperial College Press, London, 2000.